# Dynamic Gas Flow Effects on the ESD of Aerospace Vehicle Surfaces

Michael D. Hogue, PhD
NASA, Flight Technology Branch, UB-R2
Electrostatics & Surface Physics Laboratory
Kennedy Space Center, FL 32899
phone: (1) 321-867-7549
E-mail: Michael.D.Hogue@nasa.gov

Rachel E. Cox
NASA, Flight Technology Branch, UB-R2
Kennedy Space Center, FL 32899
E-mail: Rachel.E.Cox@nasa.gov

Jaysen Mulligan
University of Central Florida
Orlando, FL 32816
E-mail: mulligan2015@gmail.com

Kareem Ahmed, PhD
University of Central Florida
Orlando, FL 32816
E-mail: Kareem.Ahmed@ucf.edu

Jennifer G. Wilson
NASA, Flight Technology Branch, UB-R2
Kennedy Space Center, FL 32899
E-mail: Jennifer.G.Wilson@nasa.gov

Luz M. Calle, PhD
NASA, Applied Science Branch, UB-R3
Kennedy Space Center, FL 32899
E-mail: Luz.M.Calle@nasa.gov

*Abstract*— **The purpose of this work is to develop a version of Paschen's Law that takes into account the flow of ambient gas past electrode surfaces. Paschen's Law does not consider the flow of gas past an aerospace vehicle, whose surfaces may be triboelectrically charged by dust or ice crystal impingement while traversing the atmosphere. The basic hypothesis of this work is that the number of electron-ion pairs created per unit distance between electrode surfaces is mitigated by the electron-ion pairs removed per unit distance by the flow of gas. The revised theoretical model must be a function of the mean velocity, $v_{xm}$, of the ambient gas and reduce to Paschen's law when the gas mean velocity, $v_{xm} = 0$. A new theoretical formulation of Paschen's Law, taking into account the Mach number and dynamic pressure, derived by the authors, will be discussed. This equation was evaluated by wind tunnel experimentation whose results were consistent with the model hypothesis.**

TABLE 1: NOMENCLATURE

| | |
|---|---|
| $\alpha$ | Electron – ion pairs created per unit length |
| $\alpha'$ | Electron – ion pairs created per unit length with gas flow |
| $\beta$ | Electron – ion pairs removed per unit length by the gas flow |
| $\delta$ | Electron – ion pairs added per unit length by the gas flow |
| $n_e$ | Number of electrons |
| $n_i$ | Number of ions |
| $V_s$ | Sparking discharge voltage (V) |
| $V_i$ | Ionization potential of the ambient gas (V) |
| $L$ | Molecular mean free path at standard atmospheric pressure ($6.8 \times 10^{-6}$ cm) |
| $y_i$ | Distance an electron travels to get enough kinetic energy to ionize other particles (m) |
| $l$ | Distance available for particles to travel between collisions (mean free path, m) |
| $P_a$ | Atmospheric pressure at sea level (760 torr) |
| $P$ | Total gas pressure (torr) |
| $q_e$ | Electron charge ($1.602 \times 10^{-19}$ Coulomb) |
| $P_s$ | Ambient or static gas pressure (torr) |
| $P_{DI}$ | Incompressible Dynamic Pressure (torr) |
| $P_{DC}$ | Compressible Dynamic pressure (torr) |
| $d$ | Electrode separation (cm) |
| $d'$ | Effective electrode separation due to gas flow (cm) |
| $\gamma$ | Secondary electron emission coefficient of the electrode material |
| $v_{xm}$ | Mean velocity of the ambient gas (m/s) |
| $\gamma_a$ | Ratio of specific heat at constant pressure to the specific heat at constant volume of the mediating gas. |
| $C_P$ | Specific heat at constant pressure |
| $C_V$ | Specific heat at constant volume |
| $\forall$ | Volume ($m^3$) |
| $K$ | Kinetic energy (J) |
| $kV$ | 1000 volts |
| $\rho$ | Density ($kg/m^3$) |

# I. INTRODUCTION

We have developed a modified version of Paschen's law [1] that takes into account the flow of gas between electrically charged conductive electrodes. This work is applicable to aerospace vehicles traveling through the atmosphere where they are subject to triboelectrically induced electrostatic charge build-up and possible electrostatic discharge (ESD) damage due to dust and ice crystal impingement. Data from preliminary wind tunnel experimentation at supersonic gas velocities were found to be consistent with the basic premise of the theoretical equation.

In 2010, the Electrostatics and Surface Physics Laboratory (ESPL) at the Kennedy Space Center (KSC) performed an analysis to determine if ice crystal impingement on the exterior of the Ares I self-destruct system antenna housing would cause any electrostatic interference on the operation of the antenna [2]. In the course of the analysis, the ESPL estimated at what potential a discharge could occur if the housing was charged triboelectrically by the ice crystals at altitudes where the ambient pressure is less than that at sea level. The difficulty in doing this was that Paschen's law was derived for stationary charged surfaces in ambient gas that had no net velocity. This was not a very good fit for the physical situation of a vehicle moving rapidly through the atmosphere where the electron-ion pairs created by the electrostatic potential can be quickly removed by the gas flow. The safety of the housing to electrostatic discharge damage was eventually shown by extensive laboratory testing despite there being no appropriate theoretical model to use.

This work has the potential to relax the launch criteria for triboelectric charging due to atmospheric dust or ice crystal impingement on spacecraft surfaces. This would save considerable sums of money of up to a million U.S. dollars on launch costs if a launch scrub could be avoided, as well as better antistatic coating development based on the results of this work.

# II. THEORETICAL DEVELOPMENT

In this section we describe Paschen's Law and the derivation of a first approximation theoretical Paschen's Law equation. An initial formulation using Reynold's number was attempted first but was found to be nonviable. The theoretical equation is developed using the Mach number with the addition of compressible dynamic pressure terms [3] [4].

Paschen's law, derived in 1889 [1], is an equation that relates the sparking or breakdown voltage between two electrodes to the product of the ambient gas pressure, $P$, and the electrode separation, $d$. When the sparking voltage, $V_s$, is reached, a discharge occurs between the electrodes. Other constant parameters in Paschen's law are the ionization potential of the ambient gas, $V_i$, atmospheric pressure at sea level, $P_a$, molecular mean free path at sea level, $L$, and the secondary electron emission coefficient of the electrode material, $\gamma$. Paschen's law is shown in Eq. (1) [5]. As the electric potential builds up between the electrodes, it affects the small number of electrons and ions typically present in the air (electron-ion pairs). These particles then separate and move towards the oppositely charged electrode. On the way, they can strike and ionize other atoms and molecules thus creating a cascade of charged particles that eventually results in a sparking discharge between the electrodes.

$$V_s = \frac{\frac{V_i}{LP_a}Pd}{ln(Pd) - ln\left[LP_a ln\left(1+\frac{1}{\gamma}\right)\right]} \tag{1}$$

Our hypothesis is that the number of electron-ion pairs created per unit distance is mitigated by the electron-ion pairs removed per unit distance by the flow of gas past the electrodes. In this first approximation, we treat the pressure gradient along the vertical axis (perpendicular to the flow) as a constant. The equation must be a function of the mean velocity, $v_{xm}$, of the ambient gas and reduce to Paschen's law, Eq. (1), when $v_{xm} = 0$.

*A. Mach Number Formulation*

When an electric potential difference is set up between two electrodes, neutral gas atoms and molecules can become ionized by collisions with the ions typically present in air. These electron-ion pairs then separate with the electrons traveling toward the positive electrode and the positively charged ions moving toward the negative electrode. If the velocity of these charged particles is great enough (kinetic energy of $K \geq q_e V_i$), then other atoms and molecules will become ionized. These new electron-ion pairs will then separate and collide with other neutral particles creating what is called a cascade of charged particles rendering the mediating gas between the electrodes more conductive. This process will eventually lead to an electrostatic or sparking discharge between the electrodes.

The number of new electron-ion pairs, d$n$, can be calculated by [5]

$$\mathrm{d}n = n\alpha \mathrm{d}x \tag{2}$$

The ionization coefficient, $\alpha$, is defined as the number of electron-ion pairs created per unit distance. For flowing gas, we need to define coefficients that deal with the removal and addition of electron-ion pairs from the vicinity of the electrodes. We define $\beta$ as the electron-ion pairs per unit distance lost and $\delta$ as the electron-ion pairs per unit distance added by the gas flow. This changes equation (2) to

$$\mathrm{d}n = n(\alpha - \beta + \delta)\mathrm{d}x = n\alpha' \mathrm{d}x \tag{3}$$

Unless the ambient gas is ionized to begin with, we can neglect the effect of the $\delta$ term so Eq. (3) can be simplified.

$$\mathrm{d}n \cong n(\alpha - \beta)\mathrm{d}n \cong n\alpha' \mathrm{d}x \tag{4}$$

Separating variables, integrating over the separation of the electrodes (from 0 to $d$), and solving for the number of electrons, $n_e$, we have

$$\int_1^{n_e} \frac{\mathrm{d}n}{n} = \alpha' \int_0^d \mathrm{d}x$$

$$n_e = e^{\alpha' d} \tag{5}$$

For the number of ions, $n_i$, we subtract one from the number of electrons.

$$n_i = e^{\alpha' d} - 1 \tag{6}$$

When positive ions strike the cathode, other electrons are released and travel to the anode. The probability per ion that electrons are released is the secondary electron emission coefficient of the electrode material, $\gamma$. A self-regenerative breakdown condition is Townsend's regeneration condition [5]

$$\gamma\left(e^{\alpha' d} - 1\right) = 1 \tag{7}$$

Solving Eq. (7) for $\alpha'$ we obtain

$$\alpha' = \frac{1}{d} ln\left(\frac{1}{\gamma} + 1\right) \tag{8}$$

There are two basic assumptions required to derive Paschen's law. One, each electron, traveling a distance ($0 \le l \le d$) through an electric field $E$ between the electrodes, loses all of its kinetic energy on impact with other particles. Two, each electron can ionize a neutral particle when its kinetic energy, $q_e El$, is equal to or greater than the ionization energy, $q_e V_i$, of the mediating gas.

To get an energy $q_e V_i$, an electron must travel a distance $y_i$. The probability of this is given by [5]

$$e^{-\frac{y_i}{l}} = e^{-\frac{V_i}{El}} \tag{9}$$

where $1/l$ is the number of impacts per unit distance.

Our hypothesis is that the probability of the loss of electron ion pairs around the electrodes by the gas flow is given by a dimensionless aerodynamic term that is proportional to the gas velocity. The candidate aerodynamic function we used for this derivation is the Mach number, $M_N = v_{xm}/c$ where $v_{xm}$ is the mean gas velocity and $c$ is the speed of sound. The Mach number was chosen because it is a function of the gas velocity and is dimensionless. The number of electron-ion pairs formed per unit distance and those removed by the gas flow can be determined by Eq. (9) with the addition of a Mach number term.

$$\alpha' = \frac{1}{l} e^{-\frac{V_i}{El} - M_N} \tag{10}$$

The E-field at discharge is $E = V_s/d$ and we substitute this into Eq. (10) to get

$$\alpha' = \frac{1}{l} e^{-\frac{V_i d}{V_s l} - M_N} \tag{11}$$

Using $l = LP_a/P$ and setting Eqs. (8) and (11) equal and solving for the discharge or sparking voltage we get

$$V_s = \frac{\frac{V_i}{LP_a}(Pd)}{ln(Pd) - ln\left[LP_a ln\left(1+\frac{1}{\gamma}\right)\right] - M_N} \tag{12}$$

This theoretical model, Eq. (12), is Paschen's Law, Eq. (1), with the Mach number in the denominator. This equation meets the requirement that when $v_{xm} = 0$ it reverts to Paschen's Law.

A graph of Eq. (12) and Paschen's Law is shown in Fig. 1 for T6061 Aluminum electrodes ($\gamma = 0.035$ [6]) with an air velocity of 600 m/s (Mach 1.8) and an electrode gap of 1.0 cm.

As can be seen in Fig. 1, the addition of the Mach number to modify the number of electron-ion pairs created between the electrodes increases the resulting sparking voltage. The effect is more pronounced at lower values of *Pd*.

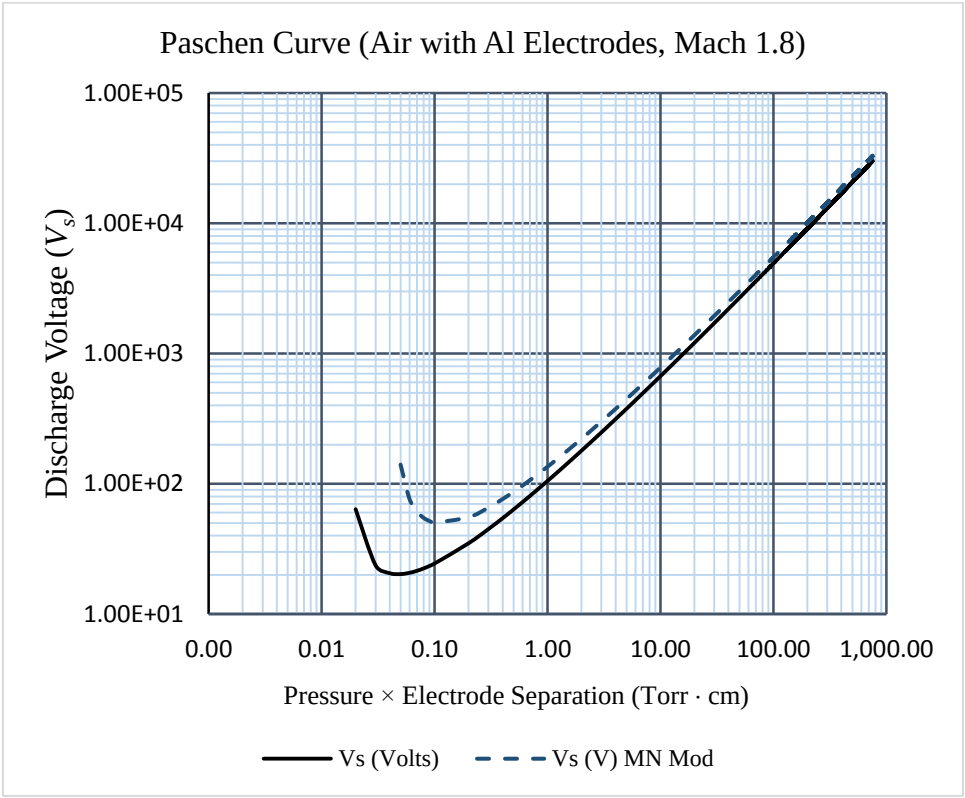


Figure 1. Paschen's Law curve compared to the theoretical model with Mach number formulation for Aluminum electrodes in air moving at Mach 1.8.

### *B. Mach number Formulation with Compressible Dynamic Pressure*

When flowing gas is considered there are two components to the pressure *P*. One is the static or ambient gas pressure, $P_s$, and the dynamic pressure. The dynamic pressure used previously [2] was the incompressible dynamic pressure.

$$P_{DI} = \frac{1}{2}\rho v_{xm}^2 \tag{13}$$

Here $\rho$ is the gas density and $v_{xm}$ is the mean gas velocity. Total pressure is given by

$$P = P_s + P_{DI} \tag{14}$$

During the course of this project, we discovered that the compressible form of dynamic pressure must be used above Mach 0.3 [3]. Compressible dynamic pressure is given by [7]

$$P_{DC} = P_{DI}\left[\left(1 + \frac{\gamma_a - 1}{2} M_N^2\right)^{\frac{\gamma_a}{(\gamma_a - 1)}} - 1\right]\frac{2}{\gamma_a M_N^2} \tag{15}$$

Here $\gamma_a$ is the ratio of specific heats for the gas (air: $\gamma_a = C_P/C_V = 1.4$). The incompressible dynamic pressure, Eq. (13), can be rewritten in terms of $\gamma_a$ and the Mach number as

$$P_{DI} = \frac{1}{2}\rho v_{xm}^2 = \frac{1}{2}\gamma_a M_N^2 P_s \tag{16}$$

Substituting Eq. (16) into Eq. (15) and collecting terms we have

$$P_{DC} = P_s\left[\left(1 + \frac{\gamma_a - 1}{2} M_N^2\right)^{\frac{\gamma_a}{\gamma_a - 1}} - 1\right] \tag{17}$$

Substituting Eq. (17) into Eq. (12) we have for the sparking voltage (with $P = P_s + P_{DC}$)

$$V_s = \frac{\frac{V_i}{LP_a}\left(1+\frac{\gamma_a - 1}{2} M_N^2\right)^{\frac{\gamma_a}{\gamma_a - 1}} P_0 d}{ln\left[\left(1+\frac{\gamma_a - 1}{2} M_N^2\right)^{\frac{\gamma_a}{\gamma_a - 1}} P_0 d\right] - ln\left[LP_a ln\left(\frac{1}{\gamma}+1\right)\right] - M_N} \tag{18}$$

When $v_{xm} = 0$, Eq. (18) also reduces to Paschen's law as required. This equation is graphed in Fig. 2 for stainless steel (SS) electrodes ($\gamma = 0.02$, [6]) at various Mach numbers for air ($\gamma_a = 1.4$) between 0.5 and 3.75 and an electrode gap of 1.3 cm.

This result looks promising since the separation of the curves is more pronounced at higher pressures. This will make the differentiation of the two curves from experimental data easier. Also of note is that the minimum sparking voltage is now a function of the Mach number as well as pressure and electrode separation.

$$V_s = f(P, d, M_N) \tag{19}$$

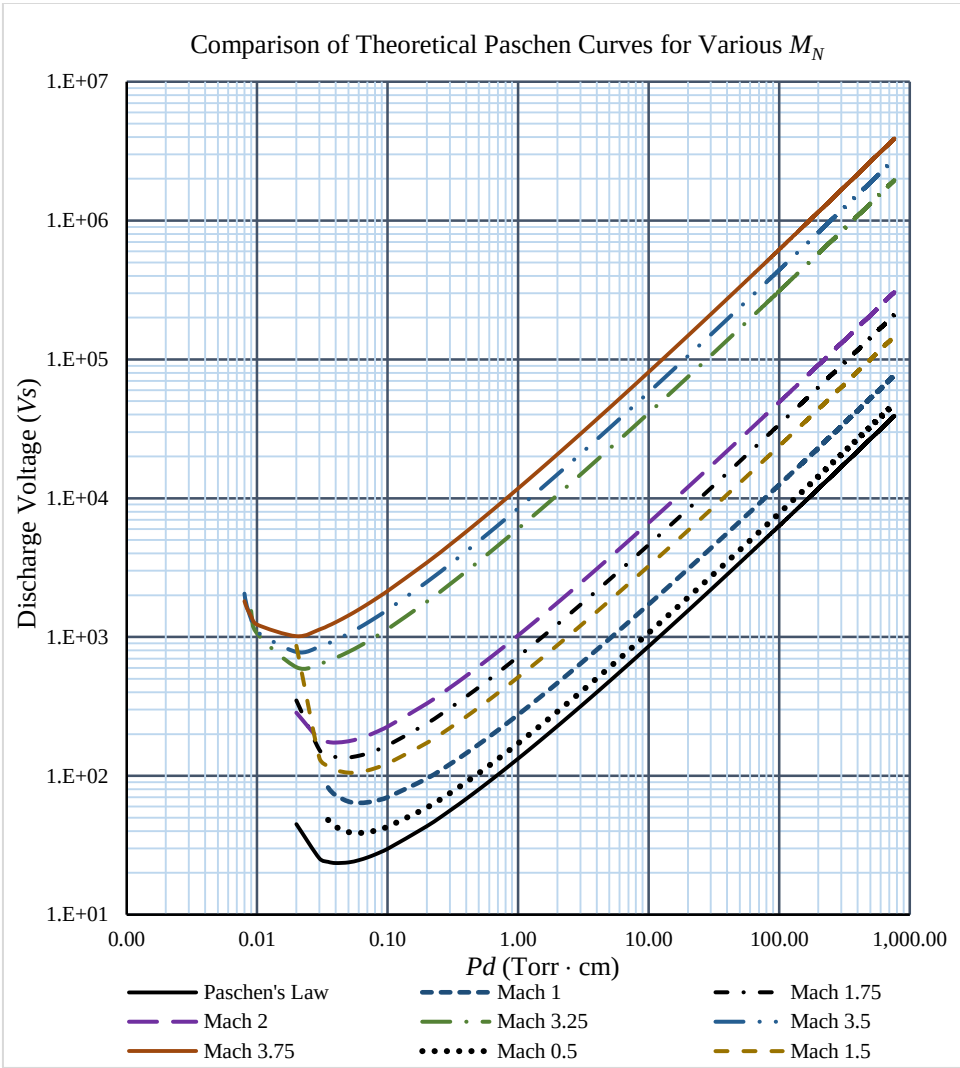


Figure 2. Graphs of the model equation, Eq. (8), for various values of the Mach number. Stainless steel electrodes in air ($\gamma_a$ = 1.4), $d$ = 1.3 cm. All theoretical curves show higher sparking voltages than the Paschen's law curve.

### *C. An Apparent Effective Discharge Path*

When air flows in a channel, a velocity profile is created [8]. This velocity profile is typically parabolic in shape with zero velocity at the channel walls and is maximum at the channel center. Velocity profile data from a Mach 1.47 wind tunnel experiment is graphed in Fig. 3 [9]. This velocity profile is mostly linear across the center of the 4.4 cm wide channel because the length of the test section did not allow sufficient time for the typical parabolic shape to develop.

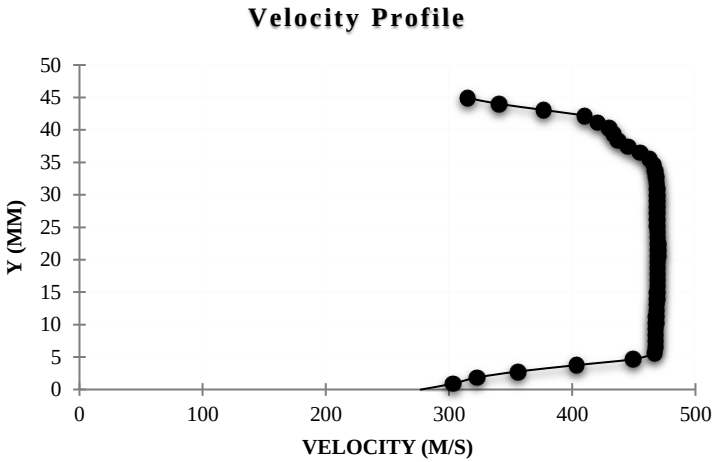


Fig. 3. Wind tunnel data with a channel width of 4.4 cm with a velocity of Mach 1.47.

Measurement of the distance along the velocity profile in Fig. 3 from a full scale printout gives approximately 11.7 cm. As described before [3] [4], from inspection of Eq. (18) we hypothesize an expression for an effective discharge path between the electrodes.

$$d' = \left(1 + \frac{\gamma_a - 1}{2} M_N^2\right)^{\frac{\gamma_a}{\gamma_a - 1}} d \tag{20}$$

For air ($\gamma_a$ = 1.4) at Mach 1.47 and $d$ = 4.4 cm, we calculate the effective electrode discharge path.

$$d' = (1 + 0.2M_N^2)^{3.5} d = 15.48\ cm \tag{21}$$

This value is 25% larger than the 11.7 cm distance graphically measured along the flow profile in Fig. 3. Analysis of other wind tunnel velocity profile data with different channel widths and Mach numbers will be necessary to better evaluate this hypothesis.

## III. Experimental Results

Wind tunnel experiments were performed at the Florida Center for Advanced Aero-Propulsion (FCAAP) of the University of Central Florida (UCF) which is a co-investigating organization of this effort. The wind tunnel facility, described previously [3] [4], was modified to allow for sparking discharges inside the test section of the tunnel.

### *A. Experiment Development*

The experiment consisted of one stainless steel electrode plate placed 1.3 cm below the upper surface of the test section in the wind tunnel. The test section, shown in Fig. 4, was modified to mount the electrode so that the upper stainless steel surface of the test section acted as the ground.

Fig. 4. Wind tunnel showing the test section (clear window on the left) and the internal sting on the right (with a standard aerodynamic cone attached) to which the electrode was mounted in this disassembled view.

The electrode plate was designed by UCF and fabricated by KSC. This plate is made from 304 SS with all edges rounded and surfaces polished to reduce field concentration points. The electrode is 2.0 cm wide by 3.0 cm long with a tapered thickness from 0.32 cm to 0.64 cm. The flat surface of the electrode was positioned to parallel the upper test section surface. A round projection off the end of the flat portion of the electrode was used to mount the electrode onto the test section sting mount and to provide for electrical connection to the power supply. The design of the electrode plate is shown in Figs. 5 and 6. Aluminum was the first electrode metal of choice, but preliminary wind tunnel tests showed that in the electrode configuration required, aluminum deflected too much to keep the gap constant during supersonic flow. A change of material to 304 stainless steel eliminated the deflection problem and also provided the same material for the electrode and ground as the upper surface of the test section is made from 304 stainless steel.

Glassman 10 kV (PS/EH10N10.0-CT) and 60 kV (PS/EH60R01.5) power supplies were used to energize the electrode with the upper surface of the stainless steel test section acting as the ground. Supply voltage was limited by the rating of the high voltage cable to 40 kV. Both voltage and current between the electrode and upper test section surface were monitored by a Tektronix DPO 4034 digital phosphor oscilloscope. The UCF facility also had Schlieren flow visualization capability to determine the shock reflections and pressures around the electrode. Also, for the experiments, discharges were recorded with GoPro™ video of the test section via the side windows. A high-level schematic of this experiment is shown in Fig. 7.

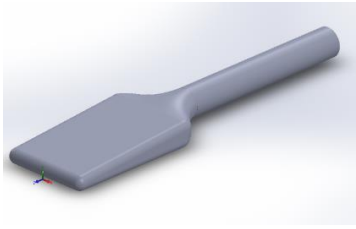

Fig. 5. 304 Stainless steel electrode design.

Fig. 6 304 Stainless steel electrode integrated into the wind tunnel sting mount. The white tube is made from polytetrafluoroethylene (PTFE), which is an insulator. The copper tube provides structural support.

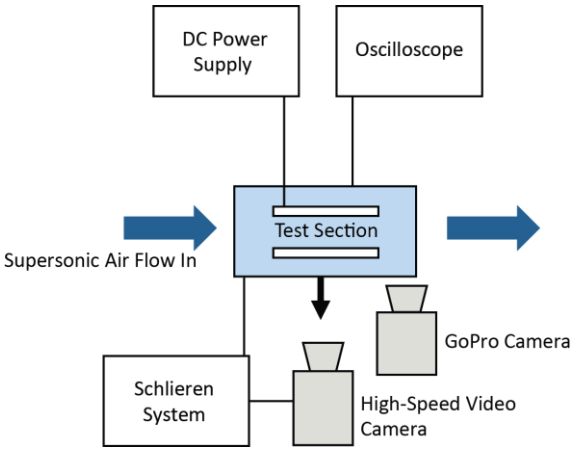


Fig. 7. High level schematic of the wind tunnel experiment to measure the electrical discharge characteristics of high-speed flow past electrodes.

### *B. Experiments, Data, and Analysis*

Two types of experiments were performed using the apparatus described in Section III-A. One experiment was to start the wind tunnel and, under steady supersonic flow, ramp up the electrode voltage to observe any sparking. The sting mount could not position the electrode closer than 1.3 cm to either surface of the test section. Also, the dimensions of the cable path through the sting mount precluded the use of high voltage wires above 40 kV in rating. The electrode was preloaded to approximately 10 kV, which is below the sparking voltage, so that the ramp span would not be as large. The supersonic steady state condition only lasts for 30 seconds or less, depending on the air tank pressure and the Mach number. This made it difficult to ramp the electrode voltage in so short a time. Also, the pressure between the electrode and the upper surface of the test section was not fully consistent across the electrode because of shock reflections. Typical shock wave reflections are visible in Fig. 8, which shows a Schlieren image for the electrode under Mach 3.5 flow.

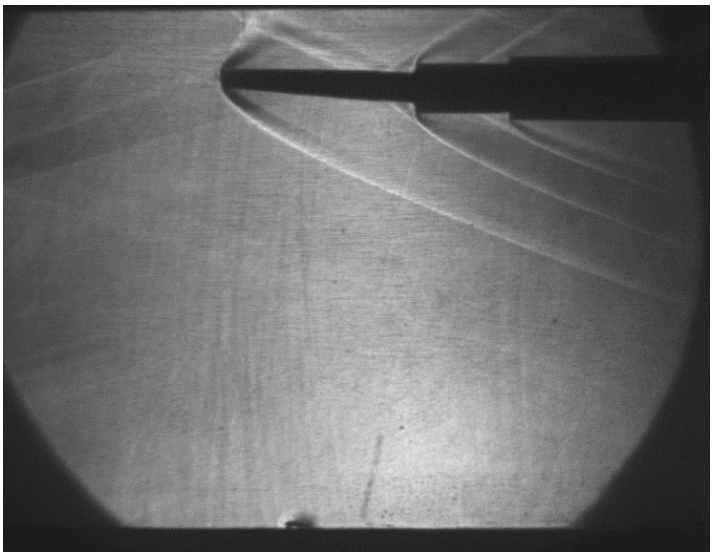

Fig. 8. Schlieren image of Mach 3.5 shock waves and reflections around the electrode. Air flow is left to right.

The second experiment involved preloading the electrode so that it sparked during no-flow conditions, then turning on the wind tunnel. The sparking would stop as soon as the air reached a sufficient velocity to reduce the number of electron-ion pairs in the gap between the electrode and the upper surface of the test section.

An example of the spark-quenching effect of supersonic air flow is shown in Fig. 9. Here we see the attainment of sparking between the electrode and the grounded upper surface of the test section prior to air flow in panel A (approximately 30 kV), the modification of the spark as air velocity increases in panel B, quenching of sparking in panel C, and the resumption of sparking when air velocity falls at the end of the run. It was noted in these experiments that prior to the quench that the shape of the spark was similar to the geometry of the velocity profile shown in Fig. 3.

The wind tunnel apparatus was modified with a more instrumented test section located to the right of the existing test section shown in Fig. 10. Here better measurement of the pressure and air flow in the test section was attained. These experiments were made at Mach 1.65, but only two experiments recorded sparks during the supersonic flow portion. These data points are shown in Fig. 11. The data points fit close to the model equation curve (Eq. 18) for air with stainless steel electrodes. Although the experimental results to date are consistent with the model hypothesis, more experimental data is required. A follow-on experiment is proposed in section IV.

## IV. Future Development Paths

Getting reliable pressure and discharge data with the experimental apparatus was found to be very difficult. Future experimental development would be in the form of a specially designed test section where both upper and lower surfaces are the electrodes and can be set at precise separations between 0.25 cm and 2.0 cm. This would allow experimental data to

be taken without the shock reflections seen using the current apparatus and give more precise pressure, velocity, and voltage measurements. A notional test section concept is shown in Fig. 12.

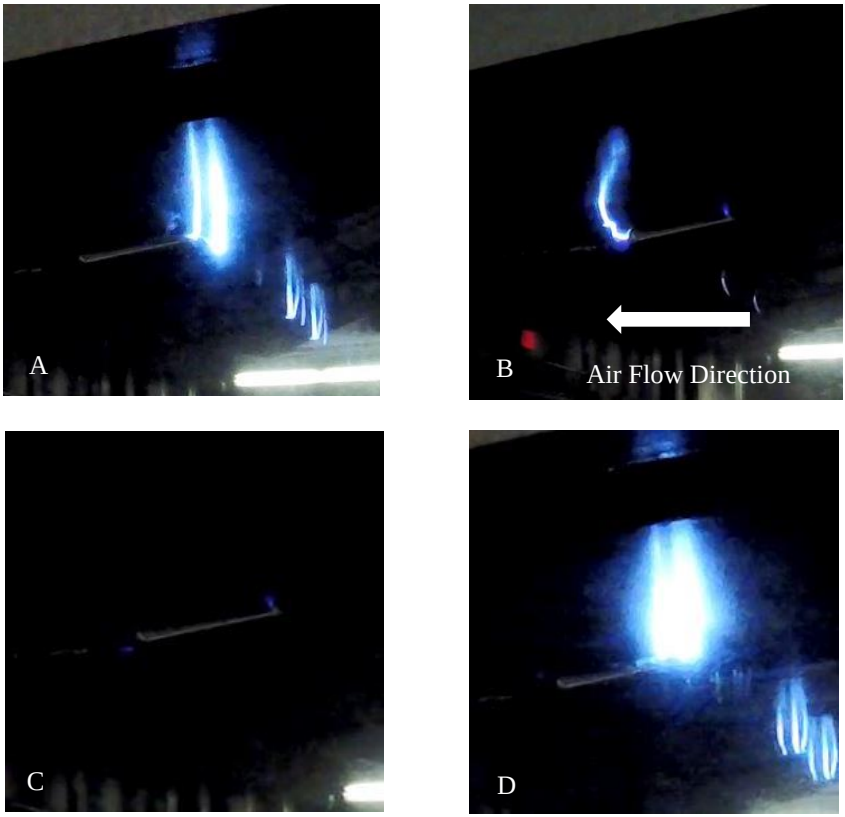


Figure 9. Photo of test section showing (A) rapid sparking before onset of air flow, (B) sparks pushed back by initial air flow towards stem of electrode, (C) sparking quenched during supersonic flow, with some small glow discharges still visible, and (D) sparking fully resumed after air flow ceased.

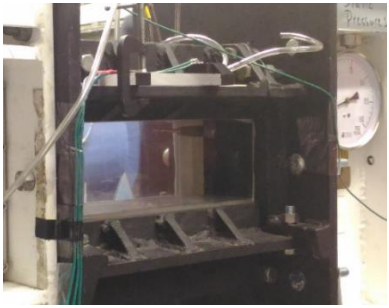

Fig. 10. New instrumented test section for the Mach 1.65 experiments.

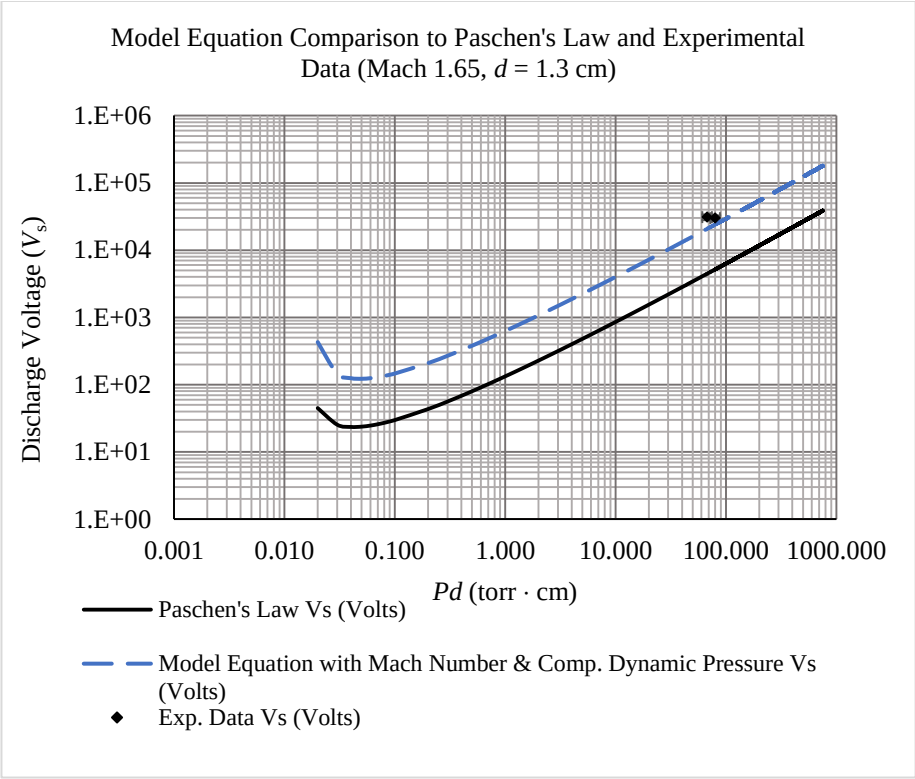


Fig. 11. Comparison of Paschen's law for a gap of 1.3 cm to the model equation with Mach number and compressible dynamic pressure terms, Eq. (18), and the two data points obtained for sparking during Mach 1.65 flow.

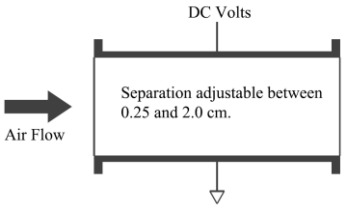


Fig. 12. Schematic concept of the proposed wind tunnel test section with the electrode and ground incorporated into the upper and lower surfaces to reduce shock reflections.

Also a LabView™ control system will be devised to automate the collection of pressure, velocity, and voltage data during wind tunnel experimentation. This will allow the collection of more precise data.

When aerospace vehicles achieve supersonic velocities, they are usually at a height where temperatures can vary greatly from sea level. The temperature dependence of both pressure and the Mach number will be theoretically investigated.

## V. Conclusion

In this paper we have presented a re-derivation of Paschen's law that takes into account the flow of gas between the electrodes as a mitigating factor on the concentration of electron – ion pairs created by the electric potential. Aerodynamic properties such as the Mach number and compressible dynamic pressure were used in this re-derivation and returned higher values of $V_s$, as would be expected if the concentration of electron – ion pairs were reduced by a rapid gas velocity. Experimental results obtained to date are consistent with the model equation though more experimentation is required. Also, in a gas flow between the electrodes, an effective discharge distance was hypothesized to be the length of the resultant velocity profile across the test section channel. Further theoretical and experimental evaluation of the model hypothesis is planned with larger and improved wind tunnel data sets.


## Acknowledgements

The authors would like to thank the NASA Science Innovation Fund (SIF) and the Kennedy Space Center (KSC) for their support. Special thanks to Dr. Carlos Calle, Mr. Michael Johansen, Mr. James Phillips, and Mr. Paul Mackey of the NASA Electrostatics and Surface Physics Laboratory (ESPL) at KSC for their reviews and helpful comments on this paper.


## References


[1] Friedrich Paschen "Ueber die zum Funkenübergang in Luft, Wasserstoff und Kohlensäure bei verschiedenen Drucken erforderliche Potentialdifferenz (On the potential difference required for spark initiation in air, hydrogen, and carbon dioxide at different pressures)". Annalen der Physik **273** (5): 69–75 (1889). *Bibcode:1889AnP...273...69P*. *doi:10.1002/andp.18892730505*.

[2] M. Hogue, C. Calle, ESPL Report, "Electrostatic Evaluation of the ARES I FTS Antenna Materials", ESPL-TR10-002, August 27, 2010. NASA, Kennedy Space Center.

[3] M. Hogue, et. al., "Dynamic Gas Flow Effects on the ESD of Aerospace Vehicle Surfaces", Proceedings, ESA Annual Meeting 2016.

[4] M. Hogue, et. al., "Revision of Paschen's Law Relating to the ESD of Aerospace Vehicle Surfaces", Proceedings, ESA 2017 Joint Conference.

[5] A. Von Hippel, *Molecular Science and Molecular Engineering*, (MIT Press, Wiley & Sons, 1959), pp 39-47.

[6] J. D. Cobine, *Gaseous Conductors: Theory and Engineering Applications*, Dover, 1993, p. 159, Table 7.3.

[7] Sultanian, Bijay, Fluid Mechanics: An Intermediate Approach, N.P.: CRC, n.d. Print, p. 33.

[8] R. W. Fox, A. T. McDonald, *Introduction to Fluid Mechanics*, 2nd ed., John Wiley & Sons, 1978, p. 496

[9] Velocity data provided by Dr. K. Ahmed/UCF, 2-17-16.